INTERNATIONAL JOURNAL OF Experimental Pathology

Int. J. Exp. Path. (2014), 95, 199–208

ORIGINAL ARTICLE

Duration of injury correlates with necrosis in caerulein-induced experimental acute pancreatitis: implications for pathophysiology

Tony G. Jacob*, Rahul Raghav†, Ajay Kumar‡, Pramod K. Garg‡ and Tara S. Roy*

**Department of Anatomy, All India Institute of Medical Sciences, New Delhi, India, †Department of Psychiatry, All India Institute of Medical Sciences, New Delhi, India and ‡Department of Gastroenterology, All India Institute of Medical Sciences, New Delhi, India*

INTERNATIONAL JOURNAL OF EXPERIMENTAL PATHOLOGY

doi: 10.1111/iep.12081

Received for publication: 18 September 2013
Accepted for publication: 3 March 2014

Correspondence:
Tara Sankar Roy
Department of Anatomy
All India Institute of Medical Sciences
Ansari Nagar
New Delhi 110029
India
Tel.: +91 1126594880
Fax: +91 1126588663
E-mails: tarasankar@hotmail.com; tsroy@aiims.ac.in

SUMMARY

Pancreatic acinar cell necrosis is indicative of severe pancreatitis and the degree of necrosis is an index of its outcome. We studied whether the dose and duration of injury correlates with severity, particularly in terms of necrosis, in caerulein-induced acute pancreatitis (AP) in Swiss albino mice. In addition to control group 1 (G1), groups 2 and 3 received four injections of caerulein every hour but were sacrificed at five hours (G2) and nine hours (G3) respectively, and group 4 received eight injections and was sacrificed at nine hours (G4). The severity of pancreatitis was assessed histopathologically and biochemically. The histopathological scores of pancreatitis in groups 3 and 4 were significantly higher than in groups 1 and 2 (4 *vs*. 1, 4 *vs*. 2, 3 *vs*. 1, 3 *vs*. 2; $P < 0.05$). TUNEL-positive apoptotic cells were significantly higher in groups 2 and 3 compared with groups 1 and 4 ($P < 0.05$). Necrosis was significantly more in group 4 than other groups (37.49% (4.68) *vs*. 19.97% (1.60) in G2; 20.36% (1.56) in G3; $P = 0.006$ for G 2 *vs*. 4 and $P = 0.019$ for G 3 *vs*. 4). Electron microscopy revealed numerous autophagosomes in groups 2 and 3 and mitochondrial damage and necrosis in group 4. The pancreatic and pulmonary myeloperoxidase activity in group 4 was significantly higher than that in the other groups ($P < 0.01$). Hence, severity of pancreatitis is a function of the dose of injurious agent, while inflammation is both dose and duration dependent, which may also explain the wide spectrum of severity of AP seen in clinical practice.

Keywords
apoptosis, autophagy, caerulein, histology, myeloperoxidase, necrosis, pancreatitis, pathology

The incidence of acute pancreatitis (AP) is increasing with significant morbidity and mortality (Su *et al*. 2006). About 25% of these patients have severe disease (severe acute pancreatitis – SAP) that has a mortality of up to 40% (Bradley 1993) and is associated with necrosis, sepsis and multiple organ failure (Sharma *et al*. 2007). The severity of AP depends on the extent of the pancreatic necrosis and correlates with organ failure and mortality (Garg *et al*. 2005).

There has been little decrease in mortality in AP because of incomplete understanding of its pathophysiology. The decrease in mortality that has been recently reported in a North American cohort study on biliopancreatic diseases requiring ERCP has been due to better selection of patients, better skills and lower incidence of open cholecystectomies (James *et al*. 2014). Due to reasons like late clinical presentation and diagnosis, unavailability of pancreatic tissue, and ethical considerations, animal models of AP are important to study the pathogenesis and test therapeutic agents (Chan & Po 2007).

The most commonly used animal model for AP is the caerulein-induced mouse model (Su *et al*. 2006). Caerulein is a cholecystokinin analogue that produces hyperstimulation of the pancreatic acinar cells at supramaximal dosage. The acute necrotizing pancreatitis produced is histopathologically similar to human AP (Van Acker *et al*. 2007). Various investigators have used different dosages for inducing

AP in this model (Lupia *et al.* 2004; Su *et al.* 2006), but the correlation of relative degrees of apoptosis and necrosis with the dose and duration of caerulein has not been well established. Apoptosis represents a milder form of pancreatitis, while necrosis is a hallmark of severe pancreatitis (Kaiser *et al.* 1995). Whether the pathophysiological changes are a function of the increasing dosage of caerulein or time duration or both has not been studied adequately.

Thus, the present study was conducted to find out whether severity of pancreatitis, relative degrees of apoptosis and necrosis and inflammation correlate with different dosages and duration of caerulein in experimental AP in mice.

Materials and methods

Animals

Experiments were performed according to the protocol approved by Animal Ethics Committee of the All India Institute of Medical Sciences, New Delhi (file number 469/IAEC/09). Adult male Swiss albino mice weighing 25–40 g were housed in shoebox cages in a standard-climate-controlled condition and were fed standard chow. The animals were fasted overnight on the day of the experiment but had free access to water.

Induction of acute pancreatitis

We induced AP by giving hourly intraperitoneal injections of caerulein (Sigma, St Louis, MO, USA), dissolved in normal saline, at a dose of 50 μg/kg/h (Chan & Po 2007). The mice were divided into four groups.

Mice of group 1 (G1, $n = 14$) were controls and received injections of equivalent volumes of normal saline. Of the 14 control animals, six animals were sacrificed at five hours and eight at nine hours.

Mice of group 2 (G2, $n = 12$) were given four injections of caerulein every hour and were sacrificed one hour after the last injection, that is, at five hours.

Mice of group 3 (G3, $n = 14$) were also given four injections of caerulein every hour but were sacrificed five hours after the last injection, that is, at nine hours.

Mice of group 4 (G4, $n = 16$) were given eight injections of caerulein every hour and were sacrificed 1 h after the last injection, that is, at 9th hour.

Groups 2 and 3 received half the dose of caerulein with respect to group 4; hence, they represent a lower dose. However, group 3, which was sacrificed at nine hours, had a longer duration of exposure to caerulein than group 2 that was sacrificed at five hours and hence would reveal whether the duration of injury affects the outcome of severity. The experiments were conducted in triplicate.

The mice were euthanized in a CO_2 inhalation chamber. The thoraco-abdominal cavity was opened, and blood was drawn from the right ventricle into heparinized syringes. The blood was centrifuged at 252 ***g*** for 5 min, and the plasma was stored at −80 °C. A portion of pancreas and lung were snap-frozen in liquid nitrogen and stored at −80 °C. The remaining pancreas, lung and kidney were immersed in 4% buffered paraformaldehyde solution for histological examination. For transmission electron microscopy (TEM), 1 mm^3 blocks of the pancreas were immersed in modified Karnovsky's solution.

We also repeated the experiments in 12 Balb/c mice with three animals in each group to study whether genetic variability affected the course of the disease.

Assessment of severity of acute pancreatitis

Histopathology. The fixed pancreas, lung and kidney tissue samples were processed for paraffin embedding, and sections were stained with standard haematoxylin and eosin. All the histopathological slides were coded by an individual not associated with the study. The histopathologist was blinded to the identity of the animal groups. Oedema, inflammation, haemorrhage and necrosis of the pancreas were graded on the basis of a well-established scoring system, where each parameter had a maximum score of 4 (Schmidt *et al.* 1992a, b). In addition, the percentage of necrotic area to the normal tissue in the sections of the pancreas was calculated using the Cavalieri probe of the image-analysis software StereoInvestigator (MicroBrightfield, Inc., Williston, VT, USA; Figure S1). This method has been standardized in our laboratory (Sharma *et al.* 2009). Sections of the lung and kidney were also scored, where the maximum score was 3 and the minimum score was 0 (Schmidt *et al.* 1992a,b).

Periodic acid–schiff staining. We stained deparaffinized sections of the pancreas with periodic acid–Schiff (PAS; Bancroft & Gamble 2008) to demonstrate the basement membrane of the pancreatic acini. Briefly, the sections were oxidized with periodic acid, then covered with Schiff reagent, washed in running tap water, and then, the nuclei were stained with Meyer's haematoxylin.

Reticular fibre staining. We stained the reticular fibres in the pancreas by the Gordon and Sweet's method (Bancroft & Gamble 2008). This not only demonstrates the basement membrane in the pancreatic tissue but also reveals the reticular connective tissue in the organ. Briefly, the sections were deparaffinized, hydrated and treated with 1% potassium permanganate solution, rinsed in tap water, bleached in 1% oxalic acid solution, washed, treated with 2.5% iron alum, washed again and then placed in silver solution. The sections were reduced in 10% formaldehyde, toned in 0.2% gold chloride solution and finally treated with 5% sodium thiosulphate solution. The sections were counterstained with neutral red.

TUNEL assay for studying apoptosis. We quantified apoptosis in the pancreatic tissue using the TUNEL assay (Bio-Vision DNA Fragmentation Assay Kit, Milpitas, CA, USA) according to the manufacturer's instructions. Briefly, the sections were deparaffinized, rehydrated, permeabilized

with proteinase-K, quenched with 30% H_2O_2 in methanol, labelled with terminal deoxynucleotidyl transferase (TdT) and Br-dUTP, and then, the Br-dUTP was detected using anti-Br-dUTP antibody and HRP-conjugated secondary antibody using diaminobenzidene (DAB) as the chromogenic agent. The sections were counterstained with methyl green. The apoptotic and the normal nuclei were counted under oil immersion objective (600X) of an Olympus BX51 trinocular microscope using an image analyser, in two different sections per animal in six different high power fields. The results were expressed as percentage of apoptotic nuclei to total number of cells counted.

Transmission electron microscopy

A portion of the pancreatic tissue was immediately immersed in modified Karnovsky's fixative (4% paraformaldehyde and 1% glutaraldehyde in 0.1 M phosphate buffer, pH 7.4). The specimens were post-fixed in 1% osmium tetroxide in 0.1 M phosphate buffer for 1–2 h, washed, dehydrated in graded series of acetone, embedded and blocked in araldite CY 212. Ultrathin sections (50–60 nm) were cut on Reichert Ultramicrotome, picked up on 300-mesh copper grids, stained with uranyl acetate and lead citrate, and viewed under a Philips Morgagni 268 D TEM (Field Emission Inc., Eindhoven, the Netherlands).

Biochemical assays

Plasma amylase measurement. Amylase levels were determined using a kinetic assay utilizing a chromogenic substrate (Genzyme, Mississauga, ON, Canada) with an ELISA plate reader (Tecan, Grödig, Austria) as has been described by Fenton *et al.* (1982).

Neutrophilic myeloperoxidase activity in the tissue. Neutrophilic myeloperoxidase activity was measured in the pancreas and lung as described by Dawra *et al.* (2008).

Total protein estimation. The tissue extract that was obtained for myeloperoxidase (MPO) estimation was also used to determine the concentration of protein in the tissue using the Bradford's assay (Sigma-Aldrich). Protein standards were made using Bovine Serum Albumin standard (Sigma P0834). To 5 µl of the standards and samples, 200 µl of Bradford's reagent (Sigma B6916) was added in a 96-well plate in triplicate. After 15 min, the absorbance was read at 595 nm using an ELISA plate reader (Tecan) at room temperature. Protein concentration (mg/ml) in the samples was computed using the standard curve.

Statistical analysis

Data are expressed as mean and standard deviation. Parametric data were analysed by one-way ANOVA with *post-hoc* Bonferroni's or Tukey's correction for multiple comparisons as appropriate. A P-value of <0.05 was taken as significant.

Results

Behaviour of the mice

The animals that received multiple injections of caerulein showed reluctance to move about in the cage compared to the controls.

Mortality

There was no mortality of the animals during the course of the experiment.

Observations during laparotomy

The animals in G2, 3 and 4 showed the presence of ascites, oedematous pancreas and visible spots of haemorrhage in the pancreas, more marked in the pancreata of G4. The lungs showed foci of spotty haemorrhage in G4. The kidneys appeared to be normal in all the groups.

Severity of acute pancreatitis

General microscopic morphology of the pancreas. Under low magnification, normal acinar cells of the pancreas showed intense bipolar staining – eosinophilic towards the lumen signifying the zymogen granules and basophilic towards the basal side, which indicated the rough endoplasmic reticulum (RER; Figure 1a). Under high magnification, there appeared to be large, round to oval, basophilic structures near the basal aspect of the cell in groups 2, 3 and 4 (Figure 1b–d). These were seen more clearly and confirmed by TEM.

Periodic acid–schiff staining. With PAS staining, the basement membrane appeared magenta and the nuclei appeared blue with PAS staining (Figure 2a). The basement membrane was seen to be intact around pancreatic acini, islets, blood vessels and ducts in all the groups except around areas of necrosis, which was seen predominantly in group 4 (Figure 2a–d).

Reticular fibre staining. The reticular fibres appear black in the stained sections, and the nuclei appear red. The normal pancreas showed acini that were well demarcated by black lines of the silver-stained reticular fibres in the basement membrane (Figure 3a). The basement membrane around the inflamed pancreatic acini (G2, 3 and 4) appeared to be diffuse, and the interacinar and intercellular oedema could be appreciated by a separation of the black lines (Figure 3b–d). Generally, the basement membrane of the pancreatic acini was intact, except around areas of necrosis (Figure 3d).

Transmission electron microscopy. The pancreas in control animals showed heterochromatic nuclei, regular parallel arrangement of the stacks of RER and zymogen granules towards the apical part of the acinar cells (Figure 4a).

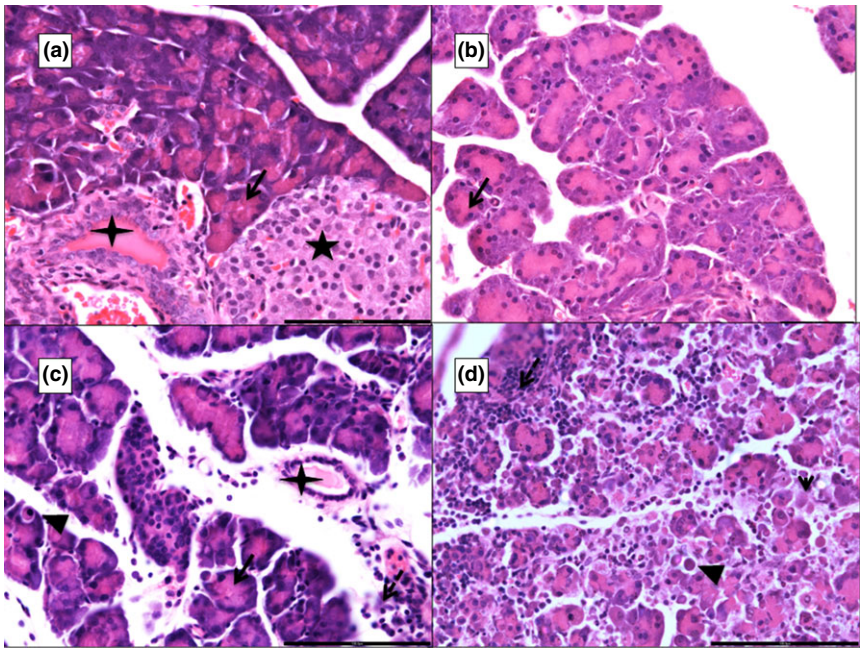

Figure 1 Photomicrographs of 5 μ thick H&E-stained paraffin sections of the pancreas. 'a' shows a control pancreas (G1) with normal acini (black arrow), islet of Langerhan (black star) and an interlobular duct (four-pointed star). 'b' from G2, 'c' from G3 and 'd' from G4 show varying degrees of interacinar and intercellular oedema, areas of necrosis (arrowhead), inflammatory infiltration (white dashed arrow; micro-abscess in 'd') and apoptosis (black arrowhead). Scale bars: a = b = c = d = 100 μm.

Numerous autophagosomes containing disintegrating membranes of the ER and zymogen granules could be seen in the animals that were given caerulein injections (Figure 4b and inset, 4c and 4d). The interstitial space was expanded due to oedema (Figure 4c,d), but the basement membrane was found to be intact except around areas of necrosis (Figure 4d). The cells were also more oedematous in G4. The RER, in these animals, was in the form of concentric whorls (Figure 4c,d). The basophilic, round structures seen in light microscopy could have been these expanded and whorled RER. Some of the nuclei showed peripheral clumping of their chromatin (Figure 4b). Cells in G3 and G4 also showed a greater number of abnormal mitochondriae.

Histopathological scoring of the pancreas. Histopathologically, the pancreas in G2 showed extensive oedema, acinar cell necrosis and moderate inflammatory infiltration but scanty haemorrhage (Figure 1b). In G3, the findings were similar to those in G2, but the number of apoptotic cells was more. In G4, the pancreas showed more extensive oedema,

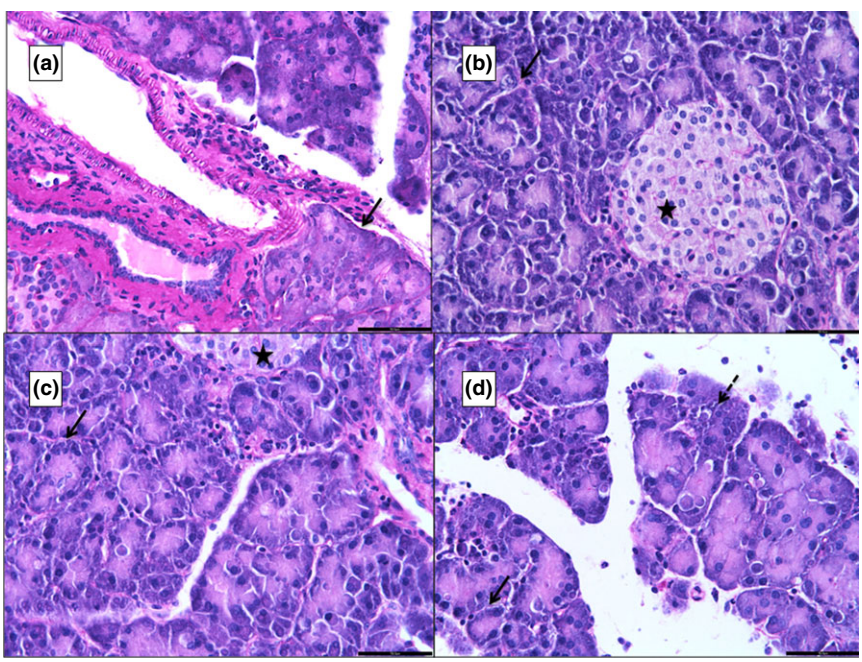

Figure 2 Photomicrographs of 5 μ thick periodic acid–Schiff (PAS)-stained paraffin sections of the pancreas. 'a' is from G1, 'b' from G2, 'c' from G3 and 'd' from G4. The black arrow points to the magenta-coloured basement membrane. 'd' shows an area of necrosis (black dashed arrow) that is not surrounded by the basement membrane. A normal islet of Langerhans is seen in 'c' (star). Scale bars: a = b = c = d = 50 μm.

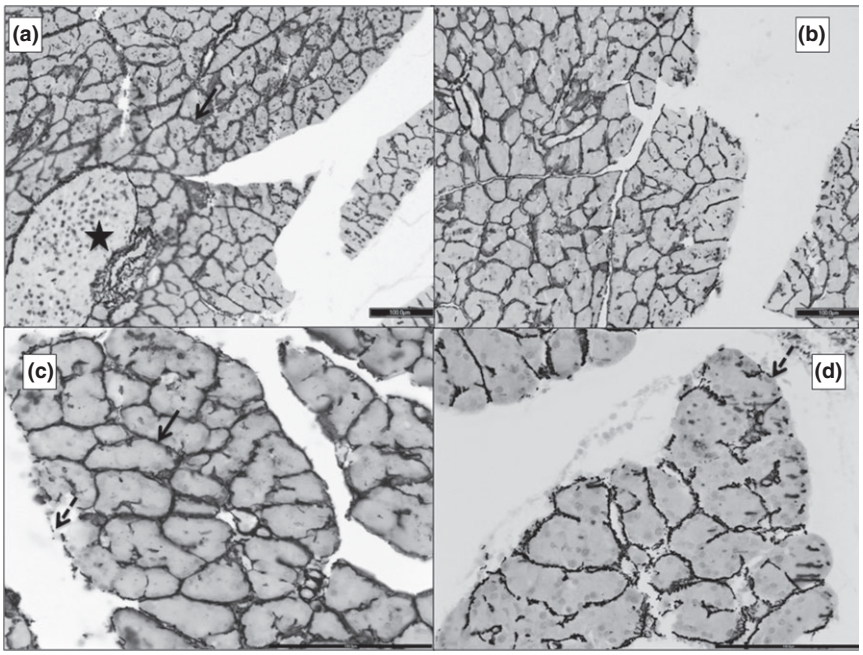

Figure 3 Photomicrographs of 5 μ thick silver-stained (Gordon and Sweet's method for reticular fibres) paraffin sections of the pancreas. 'a' is from G1, 'b' from G2, 'c' from G3 and 'd' from G4. The sections show the basement membrane as black lines (black arrows). The black lines are absent at areas of necrosis (dashed black arrow). Interacinar oedema (black arrowhead) and inflammatory infiltration (black arrow) are more prominent in 'd'. A normal islet of Langerhans is seen in 'a'. Scale bars: a = b = c = d = 100 μm.

acinar cell necrosis, inflammatory infiltration and haemorrhage as compared to either G2 or G3 (Figure 1d). The mean histological severity score of the pancreas of control animals is represented in Table 1. There was significant difference in severity of pancreatitis between all groups ($P < 0.001$).

Apoptosis and necrosis. The TUNEL-positive nuclei appeared brown, whereas those that were negative appeared green (Figure 5). The mean percentage of TUNEL-positive nuclei and the percentage of necrosis in each group are summarized in Table 1. Animals in the control group did not show any necrosis.

Histopathological scoring of the lung. In the animals with AP, the lungs showed varying degrees of collapse, congestion, haemorrhage and inflammatory infiltration around the bronchioles and blood vessels (Figure 6). The mean scores of lung injury are presented in Table 1. There was

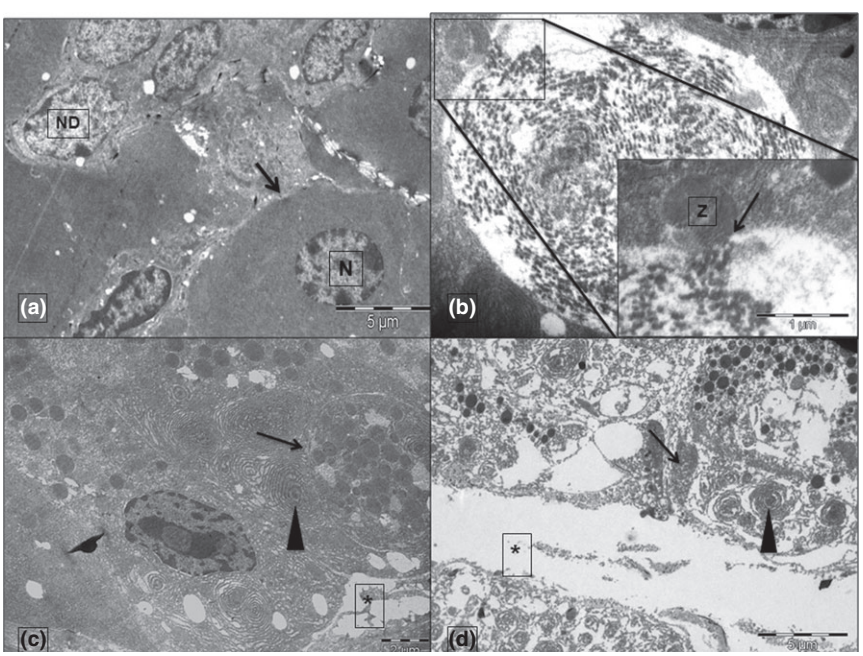

Figure 4 Transmission electron micrographs from G1 (a), G2 (b), G3 (c) and G4 (d). The nuclei of an acinar cell (N) in 'A' have been shown to be distinct from the nuclei of ductal cells (ND). The black arrows in 'a' point to the intact basement membrane that is not seen in 'd'. Asterisks (*) in 'c' and 'd' mark the interstitial oedema. Autophagosomes have been marked by arrows in 'c' and 'd'. The inset in 'b' displays the magnified view of the docking of a zymogen granule (Z) with the autophagosome (arrow). The rough endoplasmic reticulum (arrowhead) appears whorled and expanded in 'c' and 'd'. Scale bars: a = 5 μm, b = 1 μm, c = 2 μm and d = 5 μm. Inset scale bar = 1 μm.

Table 1 Summary of the various histological and biochemical parameters in different groups of animals

Parameter		Group 1	Group 2	Group 3	Group 4	*P*-values
Histopathology						
Pancreas	*N*	14	12	14	16	(1 *vs.* 2, 1 *vs.* 3, 1 *vs.* 4, 2 *vs.* 3, 2 *vs.* 4, 3 *vs.* 4 – $P < 0.001$)
	Mean (SD)	0.33 (0.05)	7.83 (1.01)	9.38 (0.78)	11.75 (1.69)	
Lung	*N*	14	12	14	16	(1 *vs.* 2, 1 *vs.* 3, 1 *vs.* 4, 2 *vs.* 3, 3 *vs.* 4 – $P < 0.01$) (2 *vs.* 4 – $P = 0.136$)
	Mean (SD)	0.10 (0.05)	1.89 (0.26)	1.04 (0.17)	2.39 (0.49)	
Kidney	*N*	14	12	14	16	(1 *vs.* 2, 1 *vs.* 3, 1 *vs.* 4, 2 *vs.* 3, 2 *vs.* 4 – $P < 0.01$) (3 *vs.* 4 – $P = 0.401$)
	Mean (SD)	0 (0)	1.07 (0.29)	1.08 (0.19)	2.01 (0.50)	
Apoptosis (TUNEL)	N	6	12	10	13	(1 *vs.* 2 – $P = 0.002$) (1 *vs.* 3 – $P = 0.005$) (2 *vs.* 4 – $P = 0.031$)
	Mean (SD)	38.51 (6.58)	50.40 (4.92)	51.89 (5.06)	43.39 (5.55)	
Percentage of necrosis	*N*	9	10	12	13	(1 *vs.* 2, 1 *vs.* 3, 1 *vs.* 4 – $P < 0.001$) (2 *vs.* 4 – $P = 0.006$) (3 *vs.* 4 – $P = 0.019$) (2 *vs.* 3 – $P = 1$)
	Mean (SD)	0 (0)	19.97 (1.60)	20.36 (1.56)	37.49 (4.68)	
MPO (U/mg of protein)						
Pancreas	*N*	12	12	14	16	(1 *vs.* 2, 1 *vs.* 4, 2 *vs.* 4, 3 *vs.* 4 – $P < 0.001$) (1 *vs.* 3 – $P = 0.003$) (2 *vs.* 3 – $P = 0.039$)
	Mean (SD)	0.46 (0.14)	5.10 (1.06)	2.38 (0.45)	12.73 (2.36)	
Lung	*N*	8	12	14	16	(1 *vs.* 2 – $P = 0.001$) (1 *vs.* 3, 1 *vs.* 4, 2 *vs.* 3, 3 *vs.* 4 – $P < 0.001$)
	Mean (SD)	1.79 (0.60)	6.24 (1.23)	15.66 (2.24)	31.23 (4.01)	
Plasma Amylase (U/ml)	*N*	9	11	14	12	(1 *vs.* 2, 1 *vs.* 3, 1 *vs.* 4 – $P < 0.001$) (2 *vs.* 3, 2 *vs.* 4 – $P = 0.001$) (3 *vs.* 4 – $P = 1$)
	Mean (SD)	1059.8 (198.33)	2257.80 (465.82)	6299.79 (1167.94)	6714.00 (757.81)	

Group 1 represents the control animals, Group 2 represents the animals that received four injections and were sacrificed at the 5th hour, animals of Group 3 received four injections but were sacrificed at the 9th hour and animals of Group 4 received eight injections and were sacrificed at the 9th hour. *N*, Number of animals; SD, standard deviation; TUNEL, terminal deoxyuridine nick end labelling; MPO, myeloperoxidase; U, units; *vs*., versus.

significant difference in scores between all the groups ($P < 0.01$) except groups 2 and 4 ($P = 0.136$; Table 1).

Histopathological scoring of the kidney. In the animals with AP, the kidneys showed varying degrees of congestion of blood vessels, interstitial oedema, haemorrhage and tubular necrosis (Figure 7). The mean scores of renal injury for the various groups are presented in Table 1. There was significant difference in scoring between all the groups ($P < 0.01$) except between groups 3 and 4 ($P = 0.401$).

Biochemical assays

Plasma amylase estimation. The mean amylase activity of the different groups is summarized in Table 1. The enzyme's activity was significantly increased in animals with pancreatitis with much higher levels seen in animals of groups 3 and 4 (Table 1). There was no significant difference in G3 and G4 ($P = 1$).

MPO activity of pancreas. The mean MPO activity in the pancreas of the different groups has been summarized in Table 1. There was significant increase in MPO activity in G2 and G4 when compared to G1 and G3. (1 *vs.* 3, $P = 0.003$; 2 *vs.* 3, $P = 0.039$; all other groups, $P < 0.001$).

MPO activity of lung. The mean MPO activity in the lung is presented in Table 1. There was significant increase in pulmonary MPO activity in G3 and 4 when compared to G 1 and 2 (1 *vs.* 2, $P = 0.001$, 1 *vs.* 3, 1 *vs.* 4, 2 *vs.* 3, 3 *vs.* 4 $P < 0.001$).

Balb/c mice. The histopathological and biochemical data that were derived from the replication of the above experiments in Balb/c mice have been summarized in the Table S1.

Discussion

In the present study, we have shown that caerulein can induce milder AP with predominance of inflammation and apoptosis, but also can produce severe pancreatitis with significant necrosis in mice. The pattern of cell injury and death was found to be a function of both the dose and duration of caerulein. Apoptosis and necrosis define mild and

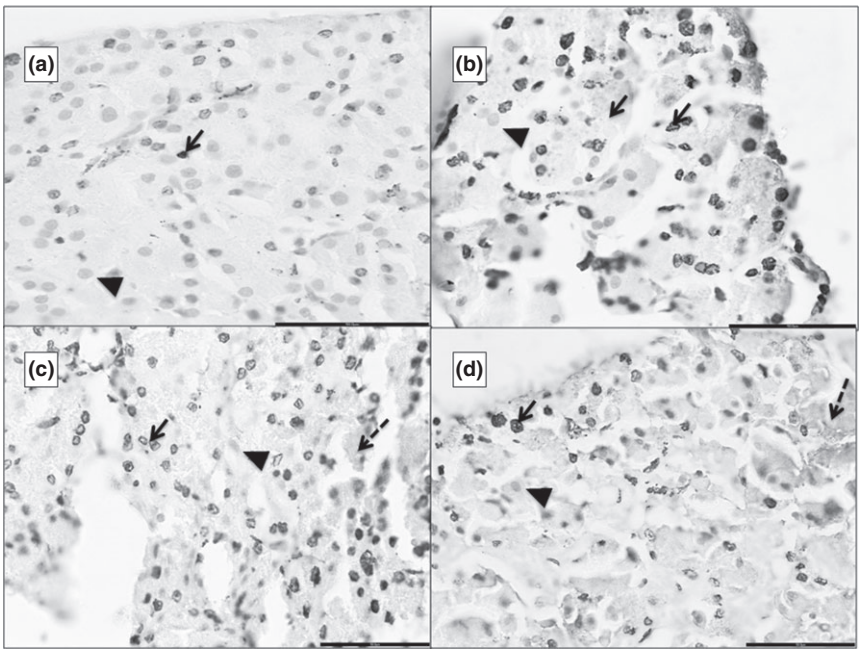

Figure 5 Photomicrographs of 5 μ thick TUNEL (terminal deoxynucleotidyl transferase deoxyuridine triphosphate nick end labelling)-stained paraffin sections of the pancreas. 'a' is from G1, 'b' from G2, 'c' from G3 and 'd' from G4. TUNEL-positive nuclei appear as dark brown dots (black arrow). The normal nuclei take up the counter-stain of methyl green (black arrowhead). There is progressively increasing necrosis from b to d (dashed black arrow). Scale bars: a = b = c = d = 50 μm.

severe forms of AP, respectively. The relative degree of apoptosis and necrosis is generally model specific. It depends on the animals and the method used to induce pancreatitis, for example caerulein induces more necrosis in the mice but apoptosis and milder pancreatitis in rats, while bile salts induce necrosis and severe pancreatitis in both mice and rats (Kaiser *et al.* 1995). Caerulein given for 4 h caused AP with apoptosis and milder systemic injury. On the other hand, the injury was much more severe with predominance of necrosis after prolonged and sustained exposure to caerulein. Both doses of caerulein produced AP although the severity of injury was significantly more in the mice that were given eight injections. This finding was in accordance with previous studies (Schmidt *et al.* 1992a,b; Kaiser *et al.* 1995). We also found that the milder form of AP produced a greater amount of apoptosis. This was also consistent with some of the earlier reports (Kaiser *et al.* 1995; Bhatia 2004a,b).

These observations suggest that there is a switch in the pattern of cell death from apoptosis to necrosis. This could be related to the specific manner in which the pancreatic acinar cells respond to noxious stimuli, both in human and

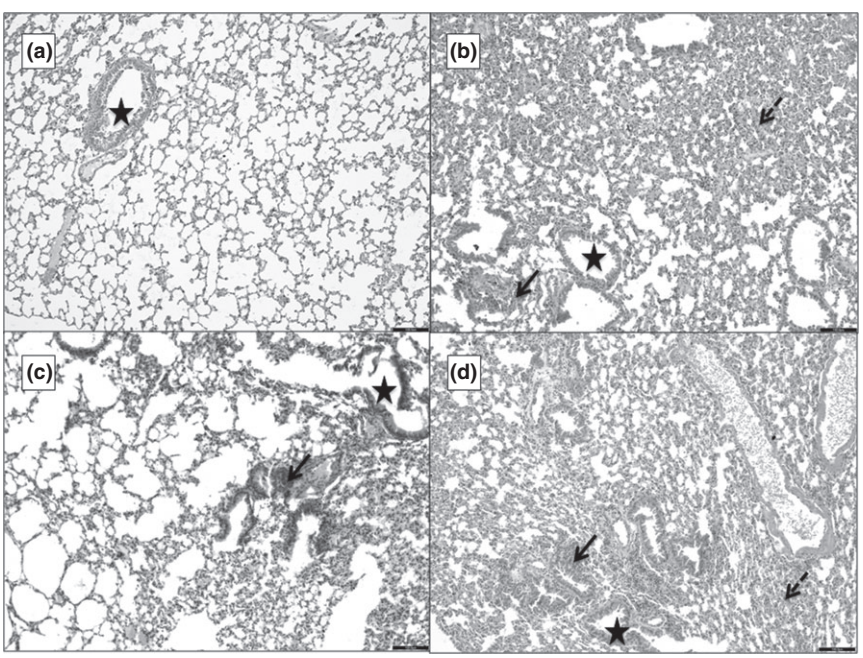

Figure 6 Photomicrographs of 5 μ thick H&E-stained paraffin sections of the lung. 'a' is the section from G1 showing a bronchiole (star) surrounded by alveoli and blood vessels. 'b' is from G2, 'c' from G3 and d from G4. b–d show different degrees of collapse, haemorrhage (dashed arrow) and inflammatory infiltration (black arrow). Scale bars = 100 μm.

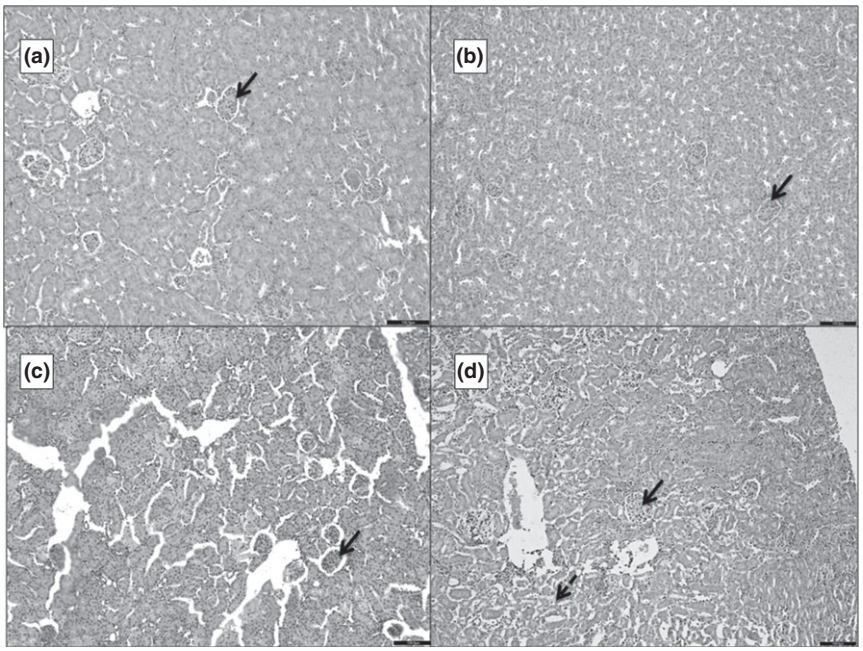

Figure 7 Photomicrographs of 5 μ thick H&E-stained paraffin sections of the kidney. 'a' is the section from G1 showing glomeruli (blue arrow) surrounded by tubules and blood vessels. 'b' is from G2, 'c' from G3 and d from G4. b–d show progressive increase in interstitial oedema and congestion of the glomeruli. 'd' also shows areas of tubular necrosis (dashed arrow). Scale bars = 100 μm.

experimental pancreatitis. With a severe injury that produces intense inflammation, the cells respond with mitochondrial injury, which promote pancreatic necrosis as evidenced by mitochondrial dysfunction (Gukovskaya & Gukovsky 2011). This is further aided by neutrophils that infiltrate the pancreas, generate reactive oxygen species (ROS) and facilitate necrosis (Abdulla *et al.* 2011). In a recent study, however, it was shown in the bile-acid induced model of AP that increased concentration of ROS in murine acinar cells (both intracellular and mitochondrial) actually led to apoptotic cell death instead of necrosis (Booth *et al.* 2011).

To find out whether the injury continued for a while even after the caerulein was stopped, that is, was injury a function of time as well, a group of mice were given only four injections of caerulein but were sacrificed after five hours, that is, at the same time as the mice that were given eight injections. Most of the histopathological and biochemical indicators of severity were fairly similar in this group to that which was given eight injections, except that the former had a lower score of lung injury, lower MPO activity both in pancreas and lung, lesser necrosis and a higher incidence of apoptosis. The continuing damage to acinar cells was also evidenced biochemically by a high plasma amylase activity. Therefore, even after the injections of caerulein were stopped, the inflammatory pathway continued but not necessarily with acute inflammatory cells (i.e. neutrophils). This inflammatory cascade also led to more apoptosis instead of necrosis. Thus even though the mice showed most of the signs of severe injury, they showed less direct and severe immediate cell death manifestoing as necrosis (Bhatia 2004a,b).

Some authors have shown that the effect of caerulein starts diminishing four to six hours after its administration (Tani *et al.* 1987; Willemer *et al.* 1992). The 5-hour wait before sacrificing the mice fell within this window and hence explains the continued injury of a lesser degree. This injury was commensurate with the degree of basement membrane injury seen with the PAS and silver staining. In the present study, the arrest of injury at four hours decreased the neutrophilic infiltration and promoted the cells to undergo apoptosis instead of necrosis that was seen with continued injurious stimulus for eight hours. This situation, of a continued injury after the insult causing AP is withdrawn, is similar to the continuing pancreatic damage that is seen in alcoholic pancreatitis even after the incident binge drinking is stopped (Gorelick 2003; Frey *et al.* 2006) and in biliary pancreatitis even after the blockage caused by the bile stone has been relieved (Lerch *et al.* 1995; Garg *et al.* 2007).

The pancreata of G4 had extensive damage to the basement membrane that was indicative of cellular disruption, which could further enhance necrosis in the pancreas due to the presence of proteolytic enzymes that can get activated at suitable pH seen in necrotic tissue (Van Acker *et al.* 2007). This observation was also confirmed by electron microscopy, wherein the mice with a later period of death after caerulein injections showed more apoptosis and autophagosomes than the other groups. The animals that were given eight injections had appreciable necrosis. This necrotic morphology has been described earlier in SAP (Kaiser *et al.* 1995). But we observed numerous autophagosomes, especially in group 3. These autophagosomes may be a method of recovery from the acute attack of AP and may explain why this group shows greater apoptosis than necrosis. The role of autophagy is now being appreciated in the pathogenesis of AP (Gukovskaya & Gukovsky 2012; Sah *et al.* 2012). What was remarkable is that we did not observe any basolateral location of zymogen granules even in the acinar cells of group 4 that had necrotic injury. These observations were similar to those made earlier by Niederau *et al.* (1985)

in caerulein-induced AP but distinctly different from what was observed by some workers in the model of alcoholic pancreatitis (Lam *et al.* 2007; Cosen-Binker *et al.* 2008). Whether the pathogenesis in these two different models is substantially different will need to be validated by further molecular studies that would examine the vesicular transport system in the pancreatic acinar cells and any disruptions therein in different models of AP.

The replication of the experiments in in-bred Balb/c mice revealed a similar pattern of histopathological and biochemical test results to what was seen in Swiss albino mice (Table S1). Hence, genetic differences alone are unlikely to change the overall effects of caerulein in producing AP.

The caerulein-induced model of AP replicates most of the pathological features of human pancreatitis although the aetiology of hyperstimulation does not resemble the usual causes of the human disease (Granger & Remick 2005; Su *et al.* 2006). However, this model has been widely and successfully used to study the pathogenetic mechanisms underlying the disease process in the pancreas (Saito *et al.* 1987; Jaworek *et al.* 2002; Saeki *et al.* 2012) and other organs that are affected by severe AP (Closa *et al.* 1999; Bhatia *et al.* 2003; Gultekin *et al.* 2007), leading to a systemic shut-down, which has a very high mortality (Beger *et al.* 1997; Baron & Morgan 1999). In addition, many therapeutic interventions for AP have been tested using this model (Demols *et al.* 2000; Frossard *et al.* 2002; Malleo *et al.* 2007). The clinical parallel of apoptosis and necrosis as shown in the present study is well known with the majority of patients having mild interstitial pancreatitis and about 20% having severe necrotizing pancreatitis (Sharma *et al.* 2007). Understanding the pathophysiological mechanisms of apoptosis and necrosis could be useful in developing therapy, which could potentially be effective in ameliorating the pancreatic injury early during the course of illness.

In summary, we have shown that the severity of AP induced by caerulein is not only dependent on dose but also on the duration of exposure. This model may be modified by dose and duration to suit the specific needs of the investigation at hand. This versatility is not available with the L-arginine, the ethionine diet induced or the surgical obstructive model of AP that are also used to evaluate interventions (Su *et al.* 2006). The switch from apoptosis to necrosis might be due to mitochondrial and other organellar dysfunction and needs further study.

This has relevance to clinical practice because the length of exposure to an agent that induces pancreatitis, like biliary stones, could augment the inflammatory cascade. This may explain the wide spectrum of clinical manifestation in terms of necrosis, apoptosis and inflammation seen in patients.

Acknowledgements

This work was supported by a grant from the Indian Council of Medical Research to PKG and TSR (No. 5/4/3-2/2009-NCD-II). The authors would also like to thank the Sophisticated Analytical Instrumentation Facility at AIIMS, New Delhi, for helping with transmission electron microscopy.

References

Abdulla A., Awla D., Thorlacius H. & Regnér S. (2011) Role of neutrophils in the activation of trypsinogen in severe acute pancreatitis. *J. Leuk. Biol.* **90**, 975–982.

Bancroft J.D., Gamble M. (2008) *Theory and Practice of Histological Techniques*, pp. 156, 171. Philadelphia, PA: Churchill Livingstone/Elsevier.

Baron T.H. & Morgan D.E. (1999) Acute necrotizing pancreatitis. *N. Engl. J. Med.* **340**, 1412–1417.

Beger H.G., Rau B., Mayer J. & Pralle U. (1997) Natural course of acute pancreatitis. *World J. Surg.* **21**, 130–135.

Bhatia M. (2004a) Apoptosis of pancreatic acinar cells in acute pancreatitis: is it good or bad? *J. Cellular Mol. Med.* **8**, c402–c409.

Bhatia M. (2004b) Apoptosis versus necrosis in acute pancreatitis. *Am. J. Physiol. Gastrointest. Liver Physiol.* **286**, G189–G196.

Bhatia M., Slavin J., Cao Y., Basbaum A.I. & Neoptolemos J.P. (2003) Preprotachykinin-A gene deletion protects mice against acute pancreatitis and associated lung injury. *Am. J. Physiol. Gastrointes. Liver Physiol.* **284**, G830–G836.

Booth D.M., Murphy J.A., Mukherjee R. *et al.* (2011) Reactive oxygen species induced by bile acid induce apoptosis and protect against necrosis in pancreatic acinar cells. *Gastroenterology* **140**, 2116–2125.

Bradley E.L. 3rd (1993) A clinically based classification system for acute pancreatitis. Summary of the International Symposium on Acute Pancreatitis, Atlanta, Ga, September 11 through 13, 1992. *Arch. Surg.* **128**, 586–590.

Chan Y.C. & Po S.L. (2007) Acute pancreatitis: animal models and recent advances in basic research. *Pancreas* **34**, 1–14.

Closa D., Sabater L., Fernández-Cruz L., Prats N., Gelpí E. & Roselló-Catafau J. (1999) Activation of alveolar macrophages in lung injury associated with experimental acute pancreatitis is mediated by the liver. *Ann. Surg.* **229**, 230–236.

Cosen-Binker L.I., Binker M.G., Wang C.C., Hong W. & Gaisano H.Y. (2008) VAMP8 Is the v-SNARE that mediates basolateral exocytosis in a mouse model of alcoholic pancreatitis. *J. Clin. Invest.* **118**, 2535–2551.

Dawra R., Ku Y.S., Sharif R. *et al.* (2008) An improved method for extracting myeloperoxidase and determining its activity in the pancreas and lungs during pancreatitis. *Pancreas* **37**, 62–68.

Demols A., Van Laethem J.L., Quertinmont E. *et al.* (2000) N-acetylcysteine decreases severity of acute pancreatitis in mice. *Pancreas* **20**, 161–169.

Fenton J., Foery R., Piatt L. & Geschwindt K. (1982) A new chromogenic amylase method compared with two established methods. *Clin. Chem.* **28**, 704–706.

Frey C.F., Zhou H., Harvey D.J. & White R.H. (2006) The incidence and case-fatality rates of acute biliary, alcoholic, and idiopathic pancreatitis in California, 1994-2001. *Pancreas* **33**, 336–344.

Frossard J.L., Bhagat L., Lee H.S. *et al.* (2002) Both thermal and non-thermal stress protect against caerulein induced pancreatitis and prevent trypsinogen activation in the pancreas. *Gut* **50**, 78–83.

Garg P.K., Madan K., Pande G.K. *et al.* (2005) Association of extent and infection of pancreatic necrosis with organ failure and

death in acute necrotizing pancreatitis. *Clin. Gastroenterol. Hepatol.* **3**, 159–166.
Garg P.K., Tandon R.K. & Madan K. (2007) Is biliary microlithiasis a significant cause of idiopathic recurrent acute pancreatitis? A long-term follow-up study. *Clin. Gastroenterol. Hepatol.* **5**, 75–79.
Gorelick F.S. (2003) Alcohol and zymogen activation in the pancreatic acinar cell. *Pancreas* **27**, 305–310.
Granger J. & Remick D. (2005) Acute pancreatitis: models, markers, and mediators. *Shock*. **24**(Suppl 1), 45–51.
Gukovskaya A.S. & Gukovsky I. (2011) Which way to die: the regulation of acinar cell death in pancreatitis by mitochondria, calcium, and reactive oxygen species. *Gastroenterology* **140**, 1876–1880.
Gukovskaya A.S. & Gukovsky I. (2012) Autophagy and pancreatitis. *Am. J. Physiol. Gastrointest. Liver Physiol.* **303**, G993–G1003.
Gultekin F.A., Kerem M., Tatlicioglu E., Aricioglu A., Unsal C. & Bukan N. (2007) Leptin treatment ameliorates acute lung injury in rats with cerulein-induced acute pancreatitis. *World J. Gastroenterol.* **13**, 2932–2938.
James P.D., Kaplan G.G., Myers R.P. *et al.* (2014) Decreasing mortality from acute biliary diseases that require endoscopic retrograde cholangiopancreatography: a nationwide cohort study. *Clin. Gastroenterol. Hepatol.* doi 10.1016/j.cgh.2013.09.054.
Jaworek J., Konturek S.J., Leja-Szpak A. *et al.* (2002) Role of endogenous melatonin and its MT2 receptor in the modulation of caerulein-induced pancreatitis in the rat. *J. Physiol. Pharmacol.* **53**, 791–804.
Kaiser A.M., Saluja A.K., Sengupta A., Saluja M. & Steer M.L. (1995) Relationship between severity, necrosis, and apoptosis in five models of experimental acute pancreatitis. *Am. J. Physiol.* **269**, C1295–C1304.
Lam P.P.L., Cosen Binker L.I., Lugea A., Pandol S.J. & Gaisano H.Y. (2007) Alcohol redirects CCK-mediated apical exocytosis to the acinar basolateral membrane in alcoholic pancreatitis. *Traffic* **8**, 605–617.
Lerch M.M., Saluja A.K., Rünzi M., Dawra R. & Steer M.L. (1995) Luminal endocytosis and intracellular targeting by acinar cells during early biliary pancreatitis in the opossum. *J. Clin. Invest.* **95**, 2222–2231.
Lupia E., Goffi A., De Giuli P. *et al.* (2004) Ablation of phosphoinositide 3-kinase-gamma reduces the severity of acute pancreatitis. *Am. J. Pathol.* **165**, 2003–2011.
Malleo G., Mazzon E., Genovese T. *et al.* (2007) Etanercept attenuates the development of cerulein-induced acute pancreatitis in mice: a comparison with TNF-alpha genetic deletion. *Shock* **27**, 542–551.
Niederau C., Ferrell L.D. & Grendell J.H. (1985) Caerulein-induced acute necrotizing pancreatitis in mice: protective effects of proglumide, benzotript, and secretin. *Gastroenterology* **88**, 1192–1204.
Saeki K., Kanai T., Nakano M. *et al.* (2012) CCL2-induced migration and SOCS3-mediated activation of macrophages are involved in cerulein-induced pancreatitis in mice. *Gastroenterology* **142**, 1010–1020.
Sah R.P., Garg P. & Saluja A.K. (2012) Pathogenic mechanisms of acute pancreatitis. *Curr. Opin. Gastroenterol.* **28**, 507–515.
Saito I., Hashimoto S., Saluja A., Steer M.L. & Meldolesi J. (1987) Intracellular transport of pancreatic zymogens during caerulein supramaximal stimulation. *Am. J. Physiol.* **253**, G517–G526.
Schmidt J., Lewandrowski K., Fernandez-del Castillo C. *et al.* (1992a) Histopathologic correlates of serum amylase activity in acute experimental pancreatitis. *Dig. Dis. Sc.* **37**, 1426–1433.
Schmidt J., Rattner D.W., Lewandrowski K. *et al.* (1992b) A better model of acute pancreatitis for evaluating therapy. *Ann. Surg.* **215**, 44.
Sharma M., Banerjee D. & Garg P.K. (2007) Characterization of newer subgroups of fulminant and subfulminant pancreatitis associated with a high early mortality. *Am. J. Gastroenterol.* **102**, 2688–2695.
Sharma V., Nag T.C., Wadhwa S. & Roy T.S. (2009) Stereological investigation and expression of calcium-binding proteins in developing human inferior colliculus. *J. Chem. Neuroanat.* **37**, 78–86.
Su K.H., Cuthbertson C. & Christophi C. (2006) Review of experimental animal models of acute pancreatitis. *HPB* **8**, 264–286.
Tani S., Otsuki M., Itoh H. *et al.* (1987) Histologic and biochemical alterations in experimental acute pancreatitis induced by supramaximal caerulein stimulation. *Int. J. Pancreatol.* **2**, 337–348.
Van Acker G.J.D., Weiss E., Steer M.L. & Perides G. (2007) Cause-effect relationships between zymogen activation and other early events in secretagogue-induced acute pancreatitis. *Am. J. Physiol. Gastrointes. Liver Physiol.* **292**, G1738–G1746.
Willemer S., Elsässer H.P. & Adler G. (1992) Hormone-induced pancreatitis. *Eur. Surg. Res.* **24**(Suppl 1), 29–39.

Supporting information

Additional Supporting Information may be found in the online version of this article:

Figure S1. Printscreen from StereoInvestigator (MBF Biosciences) to calculate the percentage area of necrosis.

Table S1. Summary of the histological and biochemical parameters in Balb/c mice.